A High Resolution Lagrangian Method Using Nonlinear Hybridization and Hyperviscosity

W. J. Rider [a,b,*], E. Love[a], G. Scovazzi[c]

[a] *Computational Shock & Multi-Physics Department, Sandia National Laboratories, MS-1323, P.O. Box 5800, Albuquerque, NM 87185-0378*

[b] *wjrider@sandia.gov*

[c] *Numerical Analysis and Applications Department, Sandia National Laboratories, MS-1319, P.O. Box 5800, Albuquerque, NM 87185-1319*

Abstract

The classical artificial viscosity method suffers from too much numerical viscosity both at and away from the shock. While some dissipation is absolutely necessary at the shock wave, it should be minimized away from the shock and disappear where the flow is smooth. The common approach to remove the unnecessary dissipation is to modify the viscosity with a limiter. We use another limiting methodology based on nonlinear hybridization, which generalizes to multiple dimensions naturally using the finite element framework. this ratio. Moreover, the properties of the limiter are to be made mesh independent through abiding by important symmetry and invariance characteristics.

We can further refine our approach with the use of hyperviscous dissipation. The hyperviscosity helps to more effectively control small-scale oscillations. The hyperviscosity can be defined by applying a symmetric filter to the viscosity. This viscosity is then combined with the original limiter. The combination of the limiter with the hyperviscosity produces sharp shock transitions while effectively reducing the amount of high frequency noise emitted by the shock. These characteristics are demonstrated computationally.

*Corresponding Author.

[1]Sandia National Laboratories is a multi-program laboratory managed and operated by Sandia Corporation, a wholly owned subsidiary of Lockheed Martin Corporation, for the U.S. Department of Energy's National Nuclear Security Administration under contract DE-AC04-94AL85000.

Keywords: Lagrangian, hydrocode, artificial viscosity, limiter, hybridization, hyperviscosity, shock wave, filter,

1. Introduction

Throughout the course of computational simulation there has been a considered battle between robust dissipative methods, and high-resolution methods providing greater accuracy, but greater risks. Lagrangian shock-hydrodynamics are no different with the classical Von Neumann-Richtmyer [1, 2] taking the role of the robust dissipative method certainly when the full theoretical values of the linear and quadratic coefficients are used [3]. By 1955, the current form of artificial viscosity had been introduced by incorporating the linear viscosity of Landhoff and Rosenbluth's suggestion to turn the viscosity off in expansion. We can then write the viscosity in its now classical form,

$$\sigma_{art}^{LO} = \rho \left[c_1 c\ell + c_2 \left\| trace\left(\mathbf{d}\right) \right\| \ell^2 \right] \mathbf{d}, \tag{1}$$

with $thevelocityis\mathbf{v}, \mathbf{d} = \text{grad}^s\left[\mathbf{v}\right]$ is the symmetric portion of the gradient,, c_1 and c_2 are positive coefficients, c is the speed of sound, ρ is the density and ℓ is a characteristic length scale for an element.

This viscosity is quite successful in capturing shocks and providing an effective dissipation for the purpose of producing entropy necessary for the physical propagation of shock waves.

The classical artificial viscosity method [2] suffers from too much numerical viscosity away from the shock where the method is absolutely necessary. The dissipation mechanism itself is detects the shock. Furthermore, the linear viscosity renders the numerical method first-order accurate (with $\ell \propto \Delta x$), where Δx is the nominal mesh specing, while the quadratic viscosity by itself is second-order preserving (with $\ell \propto (\Delta x)^2$). Each term in the viscosity has a specific role in shock propagation where the linear viscosity stabilizes the transmission of simple waves on a discrete grid while the quadratic viscosity provides dissipation for the nonlinear steepening mechanism in shock waves.

The viscosity used to capture the shock is applied to flow structures that are not shocked resulting in needless error. A common approach to defeat this issue is to modify the viscosity with a limiter [4]. The role of the limiter is to detect the presence of discontinuities, which are, which are predominantly shock waves. Traditionally, limiters used with artificial viscosity methods are based on extensions of the work of Van Leer [5] or TVD limiters [6].

These were introduced by Randy Christenson of Lawrence Livermore National Laboratory and reported in the literature by Benson [4]. The goal of the limiters is to detect regions where the flow is numerically poorly resolved and/or physical discontinuities are found. This requires the comparison of successive normalized gradients on the mesh and the limiter is triggered if the gradients are of opposite sign, or their ratio is larger than two. The method is applied multidimensionally by reducing the data into a co-linear form defined by the directions on the discrete mesh [7]. Below, we take a different approach, but establish a firmer connection between the methods in the closure.

There are several distinct origins for "limiters" including the work of Boris [8], Van Leer, Kolgan [9] and Harten and Zwas [10]. These limiters all use a nonlinear function to test the local resolution and monotonicity of the solution, and use this test to blend low- and high-order methods. Should the solution be poorly resolved or non-monotone, the low-order method is used, and if the flow is resolved and monotone, the high-order method is utilized. Most of the methods use effective logic to define the limiters as defined by Boris' minmod function. This function is written in a useful, albeit non-standard form,

$$\min \mathrm{mod}(a,b) = \tfrac{1}{4}\left[\mathrm{sgn}(a) + \mathrm{sgn}(b)\right]\left[|a+b| - |a-b|\right], \tag{2}$$

noting that this is equivalent to the standard form,

$$\min \mathrm{mod}\,(u)_j^n = \mathrm{sgn}_{j-1/2} \max\left[0, \min\left(\mathrm{sgn}_{j-1/2}\Delta_{j-1/2}u^n, \left|\Delta_{j+1/2}u^n\right|\right)\right],$$

with $\Delta_{j-1/2}u^n = u_j^n - u_{j-1}^n$ and $\mathrm{sgn}_{j-1/2} = \mathrm{sgn}\,\Delta_{j-1/2}u^n$. The minimum modulus function returns the value with the smallest magnitude if the values have the same sign, and zero if they differ. Most limited artificial viscosities use this approach. Harten and Zwas used a different approach with an algebraic switch based upon the normalized ratio of second-order differences to first-order differences.

The limiter is defined by the nonlinear hybridization technique developed in [10]. A function is defined as the normalized ratio of second-to-first derivatives, or a function of this ratio. The original method was used to define a method that merged low-order monotonic methods with high-order (non-monotonic) methods to produce non-oscillatory results near shocks (discontinuities), and high-order results away from them. The standard form is the following as applied to a flux, ,

$$u_j^{n+1} = u_j^n - \tfrac{\Delta t}{\Delta x}\left(f_{j+1/2} - f_{j-1/2}\right), \tag{3}$$

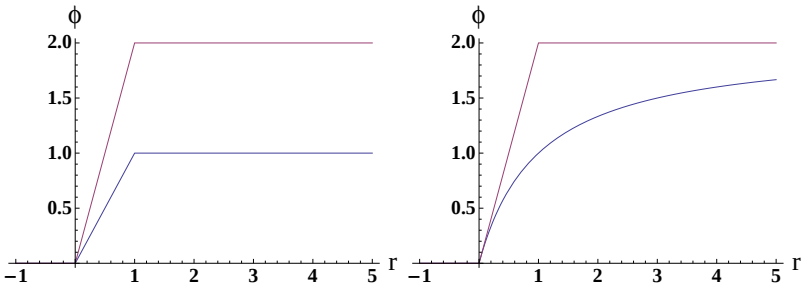

Figure 1: The limiters associated with the nonlinear hybridization plotted parametrically in the manner introduced by Sweby. The left plot shows the standard switch, which when coupled to Fromm's scheme is equivalent to a minmod limiter. The right limiter defined by the square of the standard switch is equivalent to the harmonic mean limiter when coupled with Fromm's scheme.

with Δt being the time step size and the flux is then $f_{j+1/2} = \theta_{j+1/2} f^{\text{low}}_{j+1/2} + \left(1 - \theta_{j+1/2}\right) f^{\text{high}}_{j+1/2}$ where θ is the limiter and the update is applied in conservation form. The limiter is applied in one dimension as, which gives a result that assures $0 \leq \theta \leq 1$,

$$\theta_j = \frac{\Delta x \left|\frac{\partial^2 u}{\partial x^2}\right|}{\left|\frac{\partial u}{\partial x}\right|} = \frac{|u_{j+1} - 2u_j + u_{j-1}|}{|u_{j+1} - u_j| + |u_j - u_{j-1}|}. \tag{4}$$

This is the convex combination of the low order flux, $f^{\text{low}}_{j+1/2}$ and the high order flux, $f^{\text{high}}_{j+1/2}$. Of course it is important to define the lower and high order fluxes properly in the hybridization. The low order flux, $f^{\text{low}}_{j+1/2}$, should be a monotone flux and the high flux can be chosen generally. Next, we show that this limiter forms an expression that is equivalent to the minmod limiter used in TVD methods, and the square of the limiter produces the harmonic mean (or Van Leer limiter) from [11] if the high order flux coincides with Fromm's scheme.

The demonstration of the equivalence of the two forms of limiter relies upon the algebraic form of the minmod limiter in Eqn. 2. We will show that $\left[1 - \theta\left(a, b\right)\right] \frac{a+b}{2} = \min \text{mod}\left(a, b\right)$. The equivalence between the harmonic mean form is similar, $\left[1 - \theta\left(a, b\right)^2\right] \frac{a+b}{2} = \left(|b|a + |a|b\right) / \left(|a| + |b|\right)$, These can be shown using Swebys parametric plot of the limiters with $r = a/b$ where the equivalence is obvious graphically as shown in Figure 1. The starting

point is to write the update for the scalar conservation law as

$$u_j^{n+1} = u_j^n - \frac{\Delta t}{\Delta x}\left(u_j^n - u_{j-1}^n\right) - \frac{\Delta t}{\Delta x}\left(\min \bmod (u)_j^n - \min \bmod (u)_{j-1}^n\right); v > 0.$$

We choose first-order upwind as the low-order scheme and Fromm's scheme as the high-order method. We substitute our definition for min mod, and reduce the expression algebraically to match the update for the nonlinear hybridization in Eqn. 3. We note that the equivalence only holds formally for a scalar conservation law, but the overall form is suggestive.

In the case of artificial viscosity, the limiter is applied to allow the viscosity to be modified and the usual Q takes the place of the low-order monotonic method,

$$\sigma_{art} = \theta \sigma_{art}^{LO}, \tag{5}$$

and the high-order method is the integration method without any viscosity at all. We can also use the square of the limiter to achieve a less dissipative method similar to the harmonic mean limiter.

2. Finite Element Implementation in ALEGRA

The fundamental method in the hydrocode, ALEGRA [12] is a fairly standard Q1-P0 finite element methodology. The mass and momentum equations are computed in a classical manner consistent with second-order accuracy. The method uses the standard staggered grid configuration where the velocities are at the nodes of the mesh and all the thermodynamic variables are defined at the mesh centers. The solution is defined using the finite element method using a linear function for the velocities and piecewise constant for the pressure (Cauchy stress) and energy. The artificial viscosity is introduced at element centers in either a classic scalar form (like a pressure), or a symmetric stress tensor. Most results will utilize the stress tensor approach because of its robustness on distorted meshes with strong shock waves [13]. For purposes of this paper we use a second-order predictor-corrector method introduced in [14]. Thus we have a solution that should be second-order accurate in the absence of dissipation. For the results shown here we use the tensor viscosity as our low order standard method to which we apply the limiter. Hourglass modes are damped by a Flanagan-Belytchko [15] hourglass viscosity with a coefficient set to 0.05 and multiplied by the sound speed.

The limiter is designed to detect isentropic compression, and reduce or turn off the artificial viscosity in that situation. The concept is in principle straight-forward. If the velocity field is linear, then no artificial viscosity should be applied. In multi-dimensions, the limiter is based on the Laplacian of the velocity field, which is calculated using a standard Galerkin method [16].

More precisely, define the velocity Laplacian as

$$(\nabla^2 \mathbf{v}) := \nabla(\nabla \cdot \mathbf{v}) - \nabla \times (\nabla \times \mathbf{v}) = \mathrm{div}[\mathrm{grad}[\mathbf{v}]] \; . \tag{6}$$

Then

$$\int_\Omega \boldsymbol{\eta} \cdot (\nabla^2 \mathbf{v}) \;=\; -\int_\Omega \mathrm{grad}[\boldsymbol{\eta}] \bullet \mathrm{grad}[\mathbf{v}] \;+\; \int_{\partial\Omega} \boldsymbol{\eta} \cdot \mathrm{grad}[\mathbf{v}]\; \mathbf{n} \quad \forall \boldsymbol{\eta} \; , \tag{7}$$

where Ω is the spatial domain with boundary $\partial\Omega$ and $\boldsymbol{\eta}$ is an arbitrary vector-valued function on Ω. With appropriate normalization (using the triangle inequality), this leads directly to calculation of the limiter θ_A at each node A as

$$\theta_A \;=\; \frac{\left\| -\displaystyle\int_{\Omega_A} \mathrm{grad}[\mathbf{v}]\, \mathrm{grad}[N^A] + \int_{\partial\Omega_A} \mathrm{grad}[\mathbf{v}] N^A \mathbf{n} \right\|}{\displaystyle\int_{\Omega_A} \left\| \mathrm{grad}[\mathbf{v}]\, \mathrm{grad}[N^A] \right\| + \int_{\partial\Omega_A} \left\| \mathrm{grad}[\mathbf{v}] N^A \mathbf{n} \right\|} \;\leq\; 1 \; , \tag{8}$$

where $\Omega_A = \mathrm{supp}(N^A)$, the support of the shape function N^A. The limiter is easily interpolated to element centers and applied to the artificial viscosity. If $\mathrm{grad}[\mathbf{v}]$ is a spatially constant field, then $\theta = 0$. This is easily verified by examining Equation 8. Let $\mathrm{grad}[\mathbf{v}] = \mathbf{L}$, where the tensor $\mathbf{L}$ is constant. The numerator of equation (8) in this case reduces to

$$\left\| \mathbf{L} \underbrace{\left(-\int_{\Omega_A} \mathrm{grad}[N^A] + \int_{\partial\Omega_A} N^A \mathbf{n} \right)}_{=\mathbf{0}} \right\| \; ,$$

which is identically zero by the divergence theorem.

2.1. Boundary Conditions

To ensure consistency such that the velocity Laplacian is identically zero for linear velocity fields on unstructured meshes, the boundary integral terms

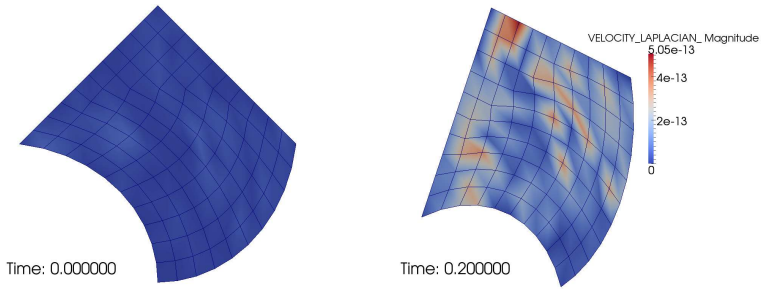

Figure 2: An image of the velocity patch test with a linear velocity field on a distorted grid. The Laplacian of the velocity should be identically zero, which is confirmed to the level of round-off error. The field is allowed to evolve under the action of the velocity field and the Laplacian continues to be approximately zero.

in equation (8) must not be omitted. Note that the boundary terms are identically zero on nodes whose support $\Omega_A = \text{supp}(N^A)$ is fully contained inside the computational domain Ω ($\Omega_A \bigcap \partial\Omega = \emptyset$). Only those nodes with support on the physical boundary ($\Omega_A \bigcap \partial\Omega \neq \emptyset$) have non-zero boundary integral terms. The capacity of the velocity Laplacian to recognize a linear field is examined in a "patch test" with the results shown in Figure 2. The formulation passes the test as the mesh deforms successfully.

2.2. Use of Filtering to Derive Hyperviscosity

Our limiter works to make the overall method less dissipative. In a number of aerospace codes the idea of adding a higher order viscosity (i.e., hyperviscosity) away from shock waves helps to keep post shock oscillations less problematic (see for example [17]). We use this idea where the shock switch (i.e., limiter) determines where the hyperviscosity is applied. One key idea is that the hyperviscosity is not applied at the shock where the lower order viscosity, the artificial or shock viscosity is applied. The hyperviscosity can help to more effectively control small-scale oscillation that invariably pollutes solutions. The hyperviscosity can be defined by applying a symmetric filter (average) to the viscosity,

$$\bar{\mathbf{d}} = \frac{1}{\text{meas}\left(\Omega_{patch}\right)} \int_{\Omega_{patch}} \mathbf{d} \mathrm{d}\Omega, \tag{9}$$

this operation could be applied recursively to produce higher order viscosities. In Figure 3 the stencil used for the filter is displayed. The hyperviscosity is

$$\sigma_{hyper} = c_3 \left[\sigma_{art}^{LO}\left(\mathbf{d}\right) - \sigma_{art}^{LO}\left(\bar{\mathbf{d}}\right)\right]. \tag{10}$$

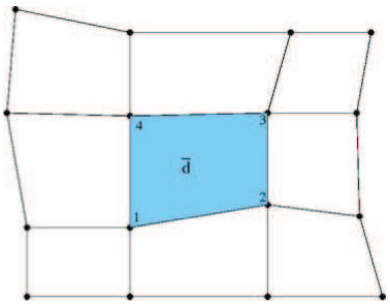

Figure 3: The stencil for the filter in two dimension is shown for the creation of a smoothed deformation field.

where the quantity $\bar{\mathbf{d}}$ is defined in Eqn. 13. This viscosity can be combined with the original limiter to produce a final form,

$$\sigma_{art} = \theta \sigma_{art}^{LO}\left(\mathbf{d}\right) + \left(1-\theta\right)\sigma_{hyper}. \tag{11}$$

The combination of the limiter with the hyperviscosity produces sharp shock transitions while effectively reducing the amount of high frequency noise emitted by the shock. Unfortunately, it is somewhat less effective with stronger shocks. These characteristics will be demonstrated computationally in the following section. Define $\bar{\mathbf{d}}$ as the mean value of the rate of deformation tensor over a patch of elements

$$\Omega_{patch} = \bigcup_{A=1}^{4} \mathrm{supp}(N^A)\ , \tag{12}$$

$$\bar{\mathbf{d}} = \frac{1}{\mathrm{meas}(\Omega_{patch})} \int_{\Omega_{patch}} \mathbf{d}\ \mathrm{d}\Omega\ . \tag{13}$$

The hyperviscosity vanishes for a linear velocity field since in that situation $\mathbf{d} = \bar{\mathbf{d}}$.

3. Results

We are going to demonstrate the methods we describe in the hydrodynamics code, ALEGRA. This will use three common test problems for shock hydrodynamics, and a flyer plate involving a complex material exhibiting non-classical shock dynamics. The common test problems are the Noh shock reflection, the Sedov-Taylor blast wave, and the Saltzmann shock reflection, all computed in Lagrangian coordinates.

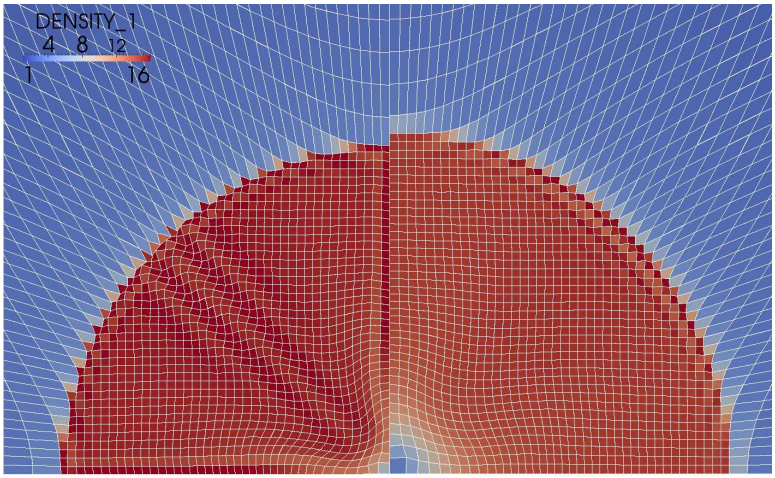

Figure 4: We examine the impact of applying the limiter to the solution of the Noh problem. On the right, we show the solution without the limiter where the shock is quite diffused, and significant wall heating results. The limited artificial viscosity shown on the left side of the figure sharpens the shock, and lessens the wall heating at the cost of the mesh quality.

3.1. Noh's Problem

The first problem to test our new viscosities on is the Noh test [18], which involves an infinitely strong reflecting shock defined in planar, cylindrical or spherical symmetry. In this case we examine the problem in cylindrical symmetry in two dimensions. The result of simply applying the limiter to the standard viscosity in Figure 4. While the shock is sharper, the mesh distortion is too large and threatens the calculation.

The action of the hyperviscosity in concert with the limiter should reduce the degree of high frequency noise allowed. Figure 5 shows this impact is shown in the one-dimensional problem computed in spherical symmetry. The hyperviscosity preserves the same basic solution, but removes the high frequency noise polluting the solution. In two dimensions the results are similar as shown in Figure 6 where the mesh distortion is significantly reduced while retaining the sharpness of the shock as compared to the original (unlimited) viscosity.

3.2. Sedov-Taylor Blast Wave

Next we present results for the Sedov problem where an idealized point explosion is computed (here using an ideal gas with $\gamma = 1.4$ resulting in an

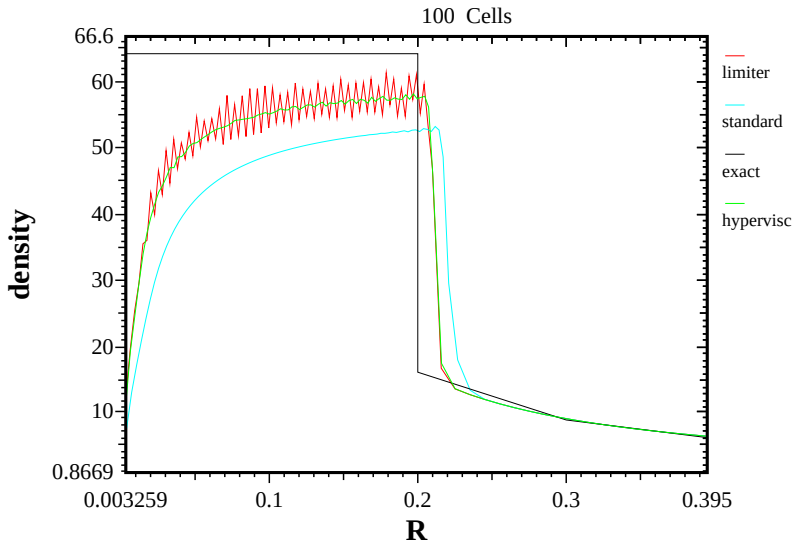

Figure 5: The spherical Noh problem in one dimension demonstrates the impact of the hyperviscosity quite succinctly. The limiter reduces dissipation, but allows oscillations, and the hyperviscosity kills the oscillations and maintains the reduced dissipation.

exact peak density of six). For brevity, we only show the solution projected onto the radial coordinate to compactly present results, and the multidimensional plots add minimal value for this problem. The solution with the limited plus hyperviscosity and unlimited artificial viscosity is shown in Figure 7. As with the Noh problem, the limiter allows for a less diffused sharper shock. Plotting the solutions as a scatter plot in distance from the origin, we can examine the solution quantitatively. The limiter allows the peak to approach the analytical result much more closely than the standard limiter, and also improves the symmetry implied by the scatter in the curves.

3.3. Saltzmann's Problem

In Figure 8 we show the results of applying the different viscosity treatments to an infinitely strong piston driven shock computed on an initially distorted mesh. This tests the stability of the method when computing a shock wave where the mesh and shock are significantly misaligned. The original viscosity does well on this problem, but at the cost of significant smearing and other dissipative effects (e.g., wall heating). The limiter sig-

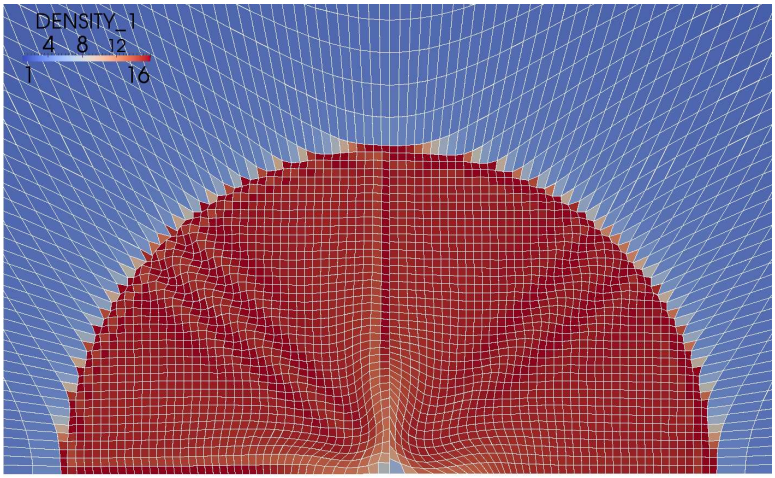

Figure 6: The use of hyperviscosity with the limiter (right) reduces the mesh distortion significantly compared with the solution using only the limiter (left). We note a slight increase in the wall heating with the use of hyperviscosity.

nificantly reduces the dissipation, but allows much greater mesh distortion. When the hyperviscosity is used together with the most aggressive limiter (θ^2) the solution quality is retained together with mesh integrity.

Another measure of the quality of the solution is the time at which the calculation fails due to element inversion. The piston can be driven continuously resulting in a series of shock reflections. This process can continue until $t = 1.0$ where theoretically infinite density would be achieved. Finite discrete calculations typically terminate prior to this. We run the problem with different artificial viscosities until the simulation terminates due to element inversion. With the original viscosity (using the original viscosity coefficients, which had been lowered to reduce diffusion) terminates at $t = 0.961$, with the larger coefficients used with a limited viscosity it terminates at $t = 0.973$. The limiter without hyperviscosity terminates significantly earlier at $t = 0.838$, the hyperviscosity returns the code to a more robust state terminating at $t = 0.949$ without the undue dissipation of the unlimited artificial viscosity.

3.4. Nonideal Equations of State

One of the aspects of using the limited artificial viscosity is greater algorithmic flexibility, for example because the limiter detects regions of smoothness in the flow. As such it is not necessary to turn off the artificial viscosity in

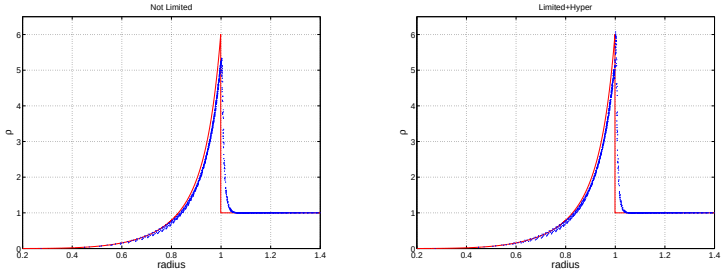

Figure 7: The Sedov-Taylor blast wave results projected into a radial coordinate showing the limited method with hyperviscosity (right) produces a high fidelity result with a good comparison to the analytical solution, and a sharp shock transition plus symmetry.

expanding flows. In the case of real materials that have regions where expansion shocks are admissible (i.e., the equation of state is locally non-convex) the artificial viscosity should be applied on expansion. Away from expansion shocks, the viscosity would be harmfully dissipative. Figure 9 shows the comparison of results. With the standard viscosity, the flow is significantly dissipated, and the expansion shock is oscillatory. On the other hand, the limiter in conjunction with the viscosity being operational in expansion is sharper and removes the oscillations from the expansion shock.

4. Summary and Conclusion

We have introduced a different form of limiting for artificial viscosity and a hyperviscosity to provide a more robust solution. This limiter can be made formally multidimensional in a FEM framework including boundary conditions. This allows it to integrate well with a hydrodynamic code written using FEM techniques. In addition we have made connections of the nonlinear hybridization to the more popular TVD methods that superseded it. This grounds the methodology in the spectrum of available methods.

In addition we have provided results from our combined methodology on a set of standard test problems to demonstrate its viability as a method. The limiter provides a substantial reduction in numerical viscosity with the cost of robustness as shown by noise in the solution and mesh distortion. The addition of hyperviscosity removes this noise effectively and controls mesh distortion returning it to the level close to that observed with the original method without the limiter.

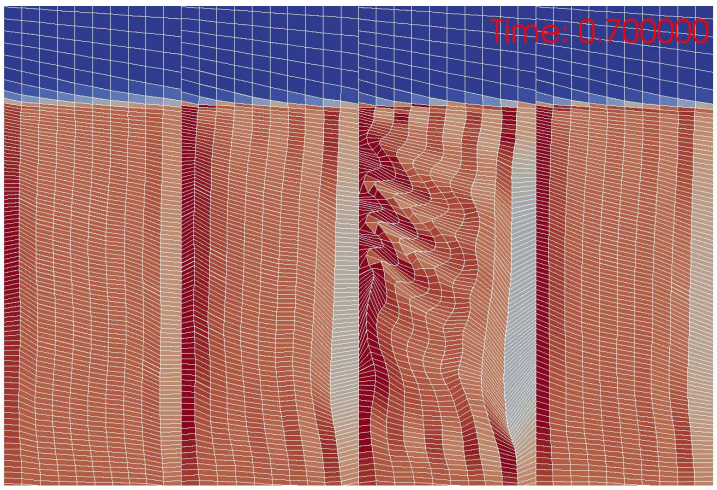

Figure 8: The Saltzmann problem demonstrating the ability of the method to resist mesh tangling. The results are shown at $t = 0.70$ The original method without limiting does well due to its overly dissipative nature. The limiter removes dissipation and the mesh tangling becomes problematic particularly for the squared form of the limiter; however the hyperviscosity provides a significant improvement in the mesh quality while retaining the sharpened shock transition.

References

[1] Richtmyer, R.D.. A proposed method for the calculation of shocks. Technical report LA-671; Los Alamos National Laboratory; Los Alamos, NM; 1948.

[2] Von Neumann, J., Richtmyer, R.D.. A method for the numerical calculation of hydrodynamic shocks. Journal of Applied Physics 1950;21:232–237.

[3] Wilkins, M.L.. Use of artificial viscosity in multidimensional fluid dynamic calculations. Journal of Computational Physics 1980;36:281–303.

[4] Benson, D.J.. A new two-dimensional flux-limited shock viscosity for impact calculations. Computer Methods in Applied Mechanics and Engineering 1991;93:39–95.

[5] Van Leer, B.. Towards the ultimate conservative difference scheme. iv. a new approach to numerical convection. J Computational Physics 1977;23:276–299.

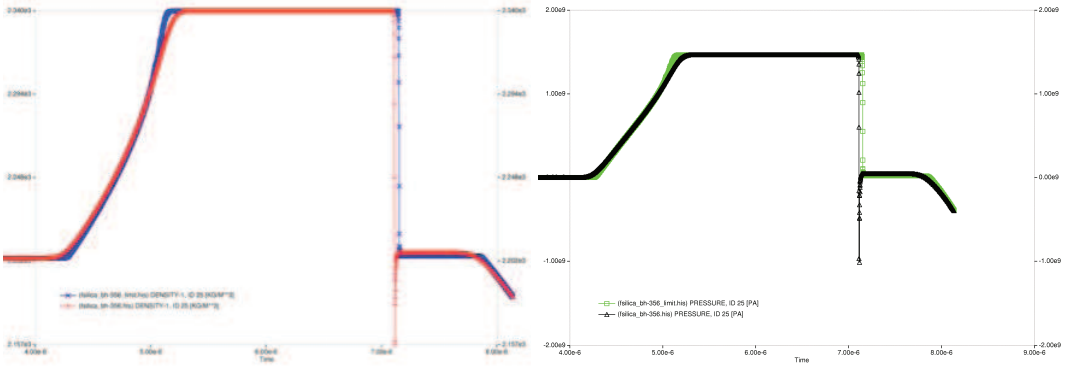

Figure 9: The silica flyer plate problem shows the behavior of the shocked plate where on release from the traversal of the non-convex region of the equation of state. The plots show the density (left) and pressure (right) at a position as time progresses. The feature at $t = 7.0e - 06$ (7 microseconds) is a large release that produces an expansion shock. Without artificial viscosity being used in the release (expansion), the shock is oscillatory. With the limiter and viscosity in expansion, the shock is sharp and non-oscillatory.

[6] Sweby, P.K.. High-resolution schemes using flux limiters for hyperbolic conservation laws. SIAM Journal of Numerical Analysis 1984;21:995–1011.

[7] Caramana, E.J., Shashkov, M.J., Whalen, P.P.. Formulations of artificial viscosity for multi-dimensional shock wave computations. Journal of Computational Physics 1998;144:70–97.

[8] Boris, J.P.. A fluid transport algorithm that works. In: Computing as a Language for Physics. Trieste, International Atomic Energy Commission; 1971, p. 171–189.

[9] Kolgan, V.P.. Application of the principle of minimum values of the derivative to the construction of finite-difference schemes for calculating discontinuous solutions of gas dynamics. Scientific Notes of TsAGI 1972;3:68–77. Reprinted in Journal of Computational Physics, Volume 230 Number 7, pp. 2384–2383, April 2011.

[10] Harten, A., Zwas, G.. Self-adjusting hybrid schemes for shock computation. Journal of Computational Physics 1972;6:568–583.

[11] Van Leer, B.. Towards the ultimate conservative difference scheme. III.

Upstream-centered finite-difference schemes for ideal compressible flow. Journal of Computational Physics 1977;23:263–275.

[12] Carroll, S.K., Drake, R.R., Hensinger, D.M., Luchini, C.B., Petney, S.V., Robbins, J., et al. ALEGRA: Version 4.6. Tech. Rep. SAND2004-6541; Sandia National Laboratories; Albuquerque, NM; 2004.

[13] Scovazzi, G., Love, E., Shashkov, M.. A multi-scale lagrangian schock hydrodynamics on q1/p0 finite elements:theoretical framework and two-dimensional computations. Computer Methods in Applied Mechanics and Engineering 2008;197:1056–1079.

[14] Love, E., Rider, W., Scovazzi, G.. Stability analysis of a predictor-corrector method for staggered-grid lagrangian shock hydrodynamics. Journal of Computational Physics 2009;228(20):7543–7564.

[15] Flanagan, D.P., Belytschko, T.. A uniform strain hexahedron and quadrilateral with orthogonal hourglass control. International Journal for Numerical Methods in Engineering 1981;17(5):679–706.

[16] Kolev, T., Rieben, R.. A tensor artificial viscosity using a finite element approach. Journal of Computational Physics 2009;228(22):8336 – 8366.

[17] Jameson, A.. Analysis and design of numerical schemes for gas dynamics 2: Artificial diffusion and discrete shock structure. International Journal of Computational Fluid Dynamics 1995;5:1–38.

[18] Noh, W.F.. Errors for calculations of strong shocks using an artificial viscosity and an artificial heat flux. Journal of Computational Physics 1987;72:78–120.